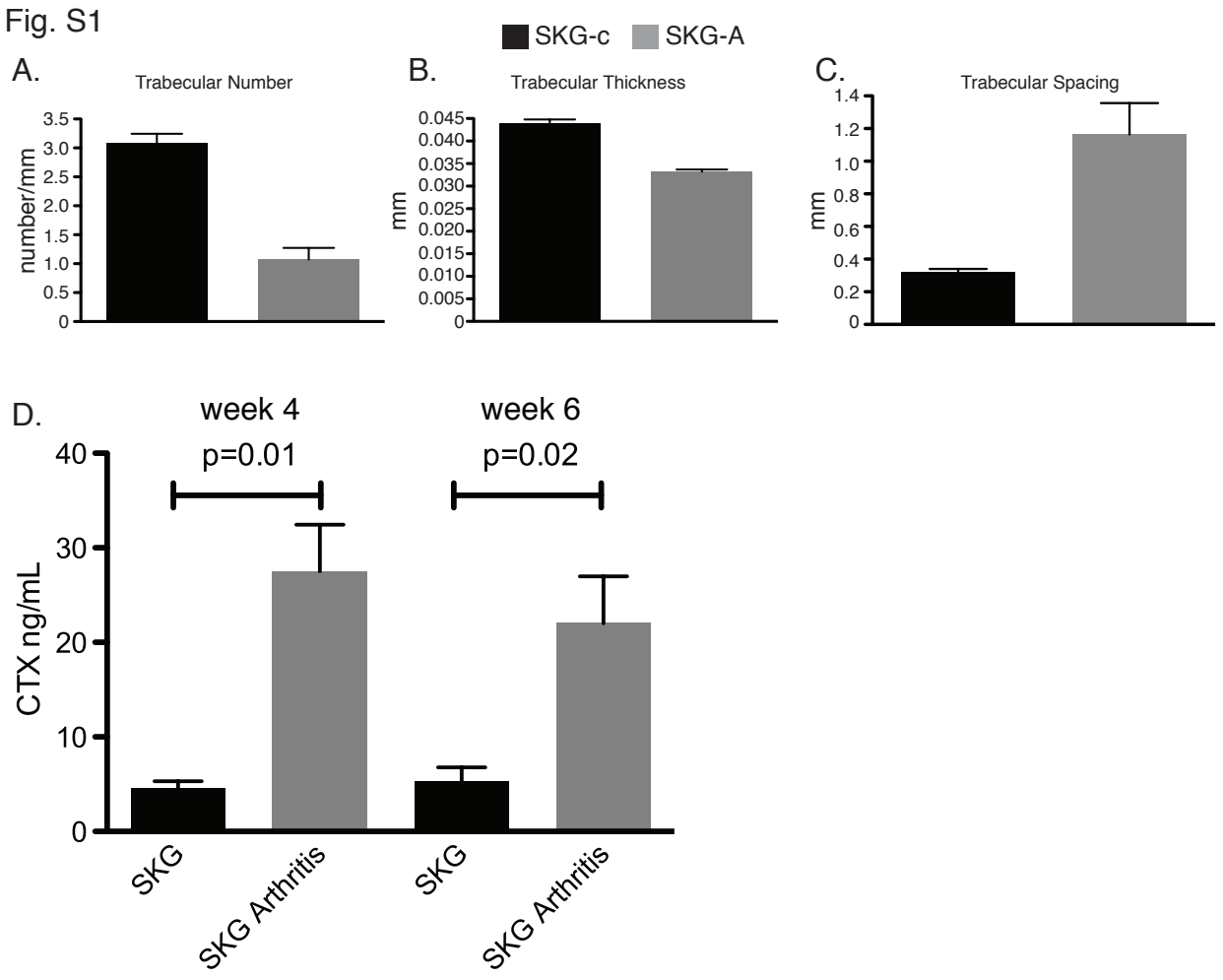

Figure S1. MicroCT analysis of SKG mice shows significant changes in proximal tibia trabecular parameter consistent with osteopenia. SKG mice at 14 weeks arthritis (SKG-A, gray bars), are compared to healthy litter mate controls (SKG-c, black bars). **(A)** Trabecular number and **(B)** trabecular thickness are significantly decreased, and **(C)** trabecular spacing is correspondingly increased in arthritic mice, $p \leq 0.04$ for all comparisons, Student's t-test. Osteoclast resorptive activity measured by serum c-telopeptide (CTX) produciton is increased at 4 and 6 weeks after zymosan injection, n=5 per group **(D)**.

Fig. S2

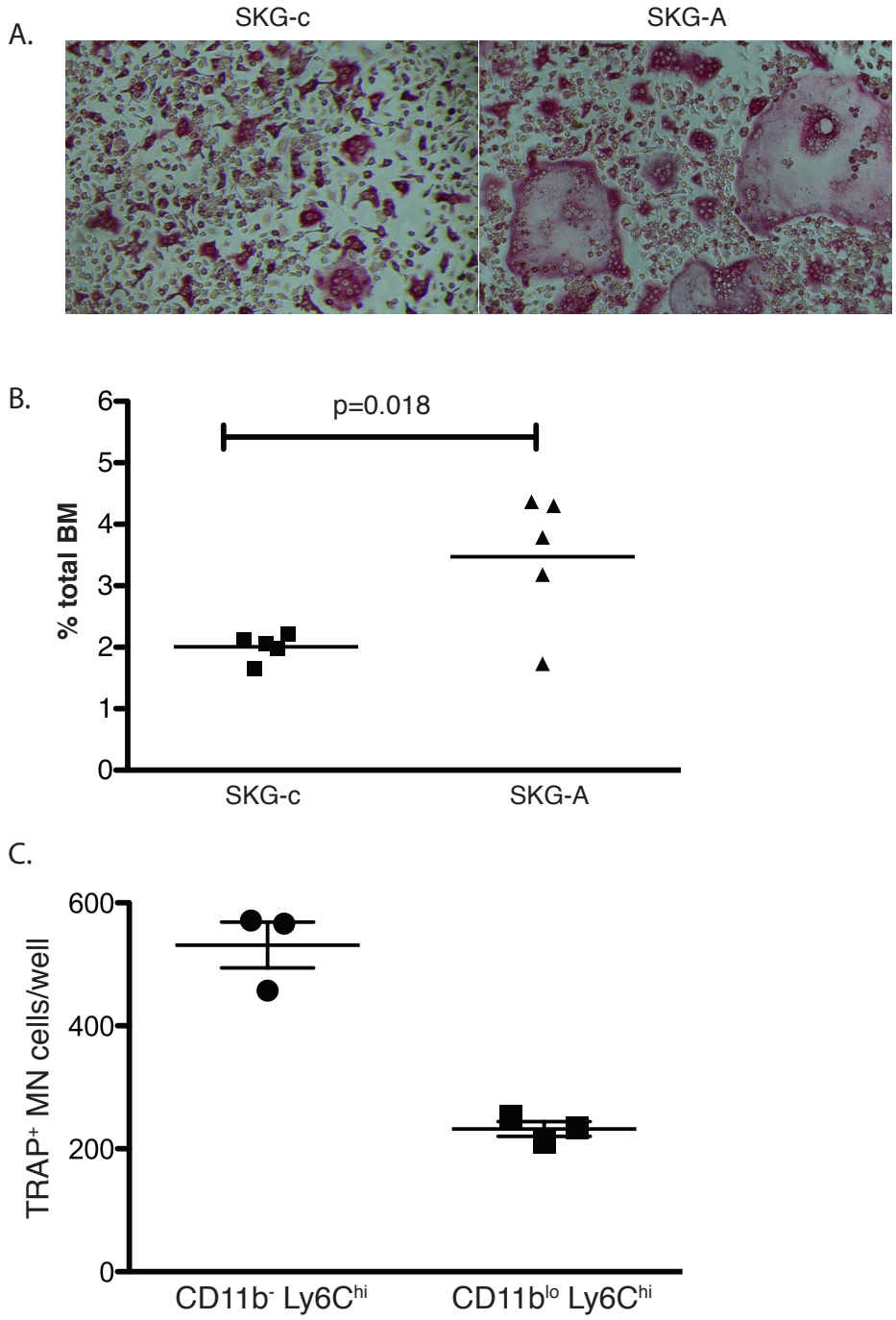

Figure S2. A. Peripheral OC differentiation increases in SKG Arthritis. Peripheral blood cells were collected from SKG mice 8 weeks after induction of arthritis (SKG-A) or from healthy SKG littermates (SKG-c), mononuclear cells were isolated by Ficoll gradeint centrifugation and plated at $1x10^5$ cells/ well in 96 well plates in 5% CMG and 25ng/mL RANKL and cultured for 7 days. Results are representative of 2 independent experiments. **B. $CD11b^{-/lo}$ $Ly6C^{hi}$ bone marrow OCP increase as early as 1 week after zymosan induction of arthritis.** CD11b and Ly6C staining of B220-CD3-Ter119- gated bone marrow from mice 1 week after zymosan injection (SKG-A) or control PBS injected mice (SKG-c) demonstrates increased OCP, n=5. Results are representative of 3 independent experiments. **C. OC precursor activity is found in both the $CD11b^-$ and $CD11b^{hi}$ $Ly6C^{hi}$ bone marrow cells.** The bone marrow $CD45R^-$ $CD3^-$ $CD11b^{-/lo}$ $Ly6C^{hi}$ population was further subdivided into $CD11b^-$ and $CD11b^{lo}$ cells and purified by fluorescence activated cell sorting. Triplicate wells

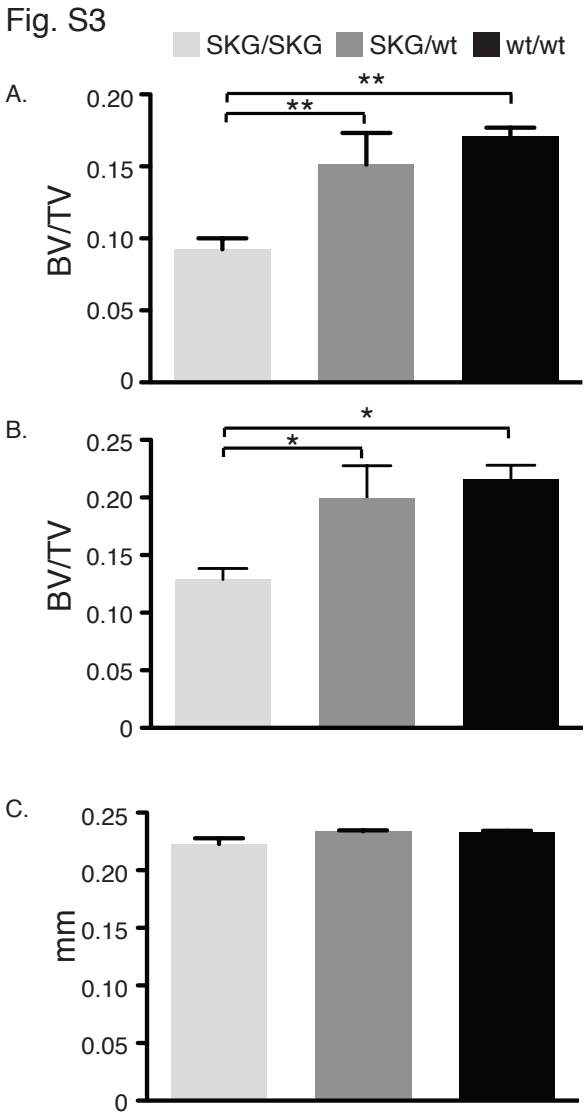

Figure S3. Female SKG mice are osteopenic compared to heterozygous and wild-type litermates. MicroCT analysis of 12-13 week old female mice from SKG^{het} x SKG^{het} parents shows trabecular osteopenia of SKG/SKG mice (light gray bars, n=6) compared to SKG^{het} (dark gray bars, n=3) and wild-type mice (black bars, n=5) at both **(A)** proximal tibia and **(B)** distal femur, ** $p \leq 0.005$, *$p \leq 0.02$, Student's t-test. **(C)** Cortical thickness, however, is not signficantly changed at this age.

Fig. S4

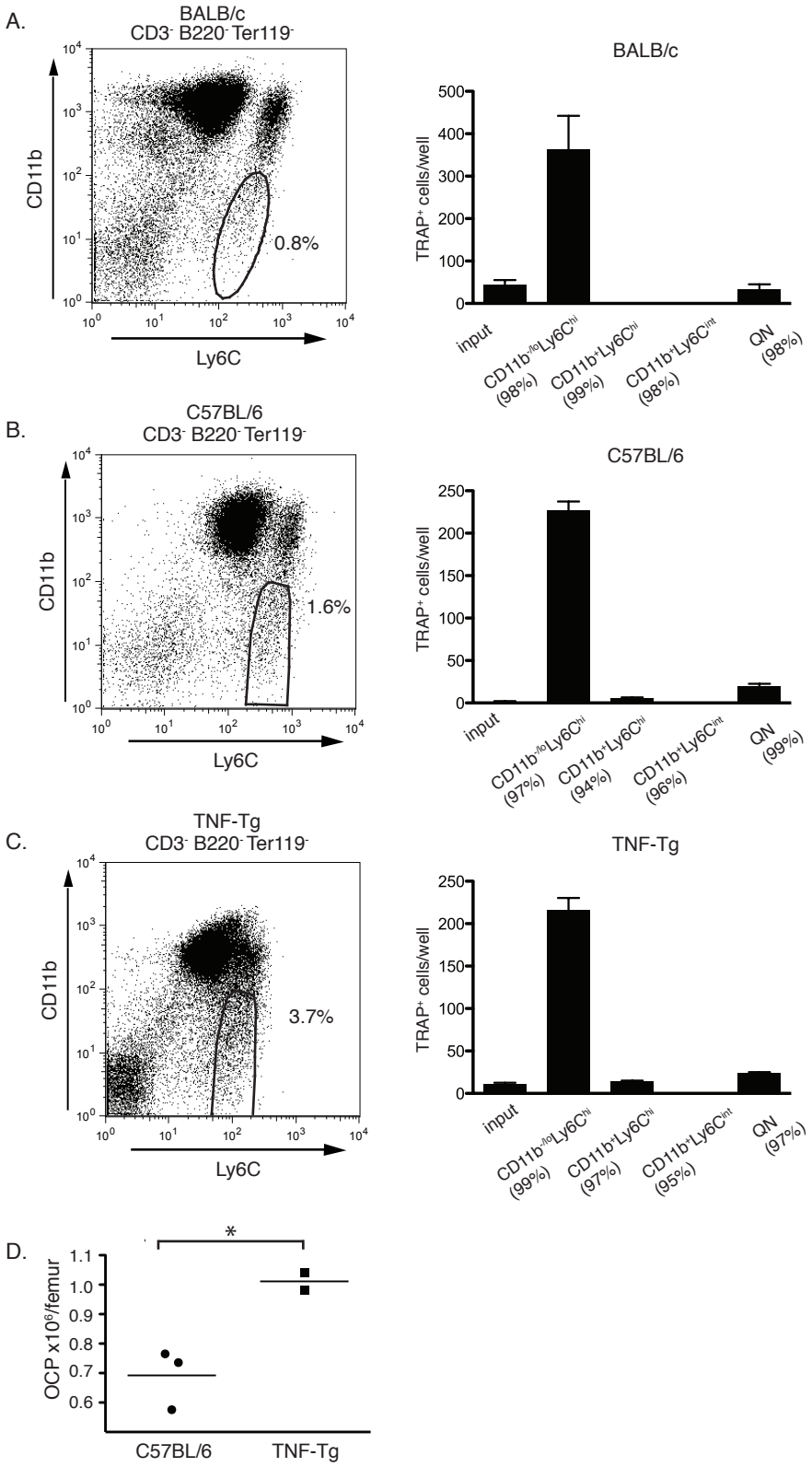

Fig. S4. CD11b$^{-/lo}$ Ly6C^{hi} OCP are the primary osteoclast precursor population independent of strain. Representative dot plots of CD11b and Ly6C stained CD3^{-}B220^{-}Ter119^{-} bone marrow and multinucleated TRAP^{+} cells cultured from individual bone marrow populations plated in triplicate for 3-4d in MCSF and 25ng/mL RANKL demonstrates that CD11b$^{-/lo}$ Ly6C^{hi} cells are also the primary osteclast precursors in **(A)** BALB/c (12.5X10^{3} cells/well) **(B)** C57BL/6 mice (2.5X10^{3} cells/well) and **(C)** 20 week old TNF-Tg mice with arthritis (2.5X10^{3} cells/well). The percent of OCP in total bone marrow is noted on the dot plot, and the purity of each sorted population is stated in parenthesis on the x-axis of the graph panel. Results are representative of 2 or more replicates. **(D)** The number of bone marrow OCP is significantly increased in arthritic TNF-Tg mice compared to age matched wild-type controls, *p=0.03.

Fig. S5

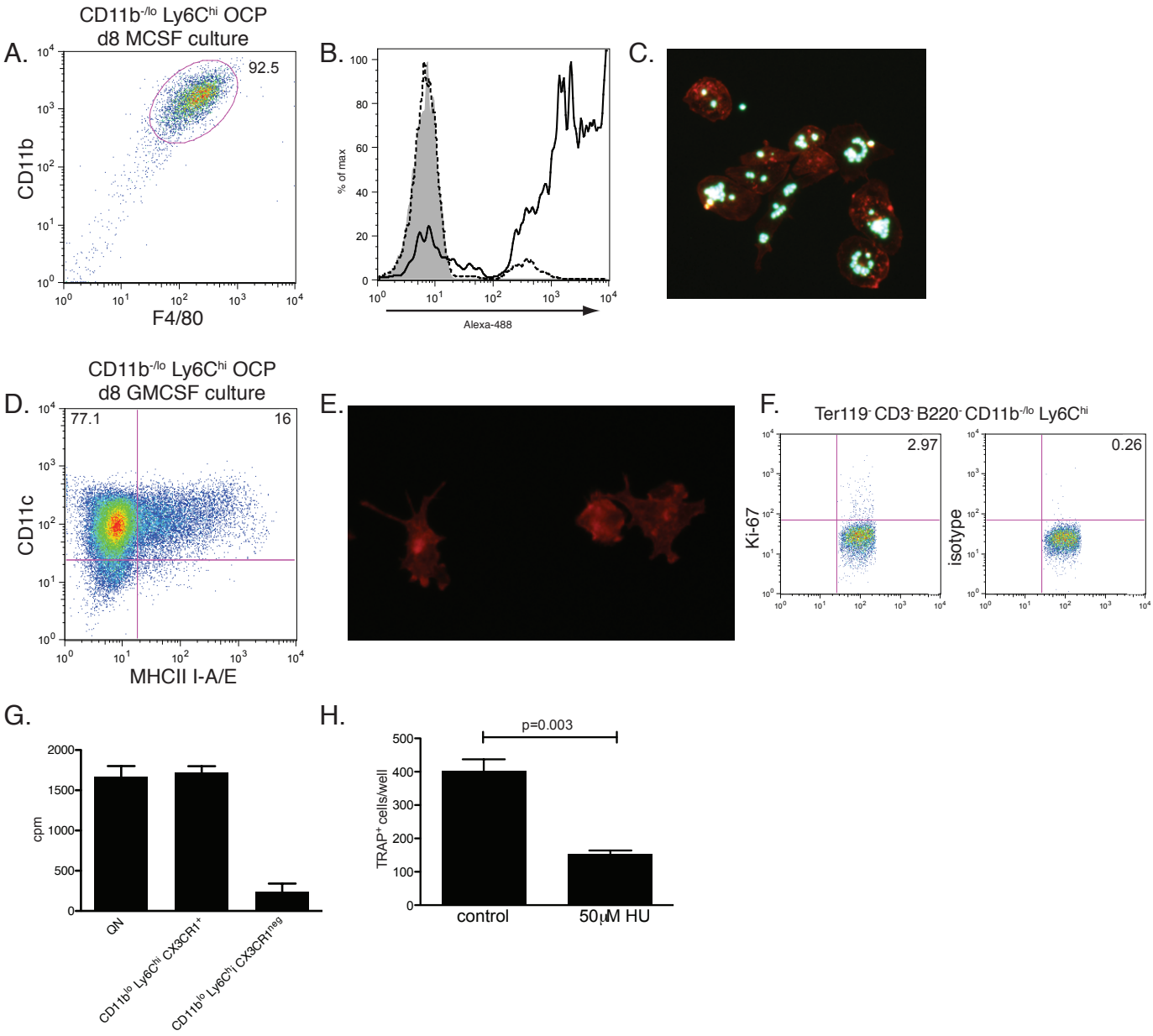

Figure S5. CD11b$^{-/lo}$ Ly6C^{hi} CD117^{+} OCP are multipotent *in vitro* and like circulating OCP are predominantly quiescent. (A-C) In the presence of MCSF, sorted CD11b$^{-/lo}$ Ly6C^{hi} CD117^{+} OCP differentiate into CD11b^{hi} F4/80^{+} macrophages with phagocytic activity. (A) After 8d culture in MCSF, OCP-derived cells are essentially all CD11b^{hi} F4/80^{+}. (B) OCP-derived macrophages phagocytose Alexa-488 labelled zymosan A and become Alex-488+ (solid line) compared to untreated cells (solid gray); uptake is blocked by preincubation with cytochalasin D (dashed line). (C) OCP-derived macrophages from (B) stained with rhodamine-phalloidin demonstrating intracellular Alexa-488 zymosan A particles, 20X. (D-E) Sorted CD11b$^{-/lo}$ Ly6C^{hi} CD117^{+} OCP differentiate into CD11c^{+} dendritic cells in the presence of GMCSF. (D) OCP cultured in GMCSF for 8d and stimulated with LPS for 4h differnentiate into CD11c^{+} cells that express MHCII^{+} in response to LPS. (E) Rhodamine-phalloidin staining of the cells in (D) demonstrates typical dendritic mophology, 20X. (F) Staining for Ki-67 demonstrates that the CD11b$^{-/lo}$ Ly6C^{hi} population is predominantly quiescent on isolation. (G) ^{3}H thymidine uptake shows that CD11b$^{-/lo}$ Ly6C^{hi} CX$_{3}$CR1^{+} OCP proliferate in response to MCSF in contrast to the CX$_{3}$CR1^{-} subpopulation. (H) Treatment with (HU) hydroxyurea greatly reduces TRAP^{+} multinucleated OC differentition from CD11b$^{-/lo}$ Ly6C^{hi} OCP, suggesting that proliferation is required for OC differentiation from bone marrow OCP.

Fig. S6

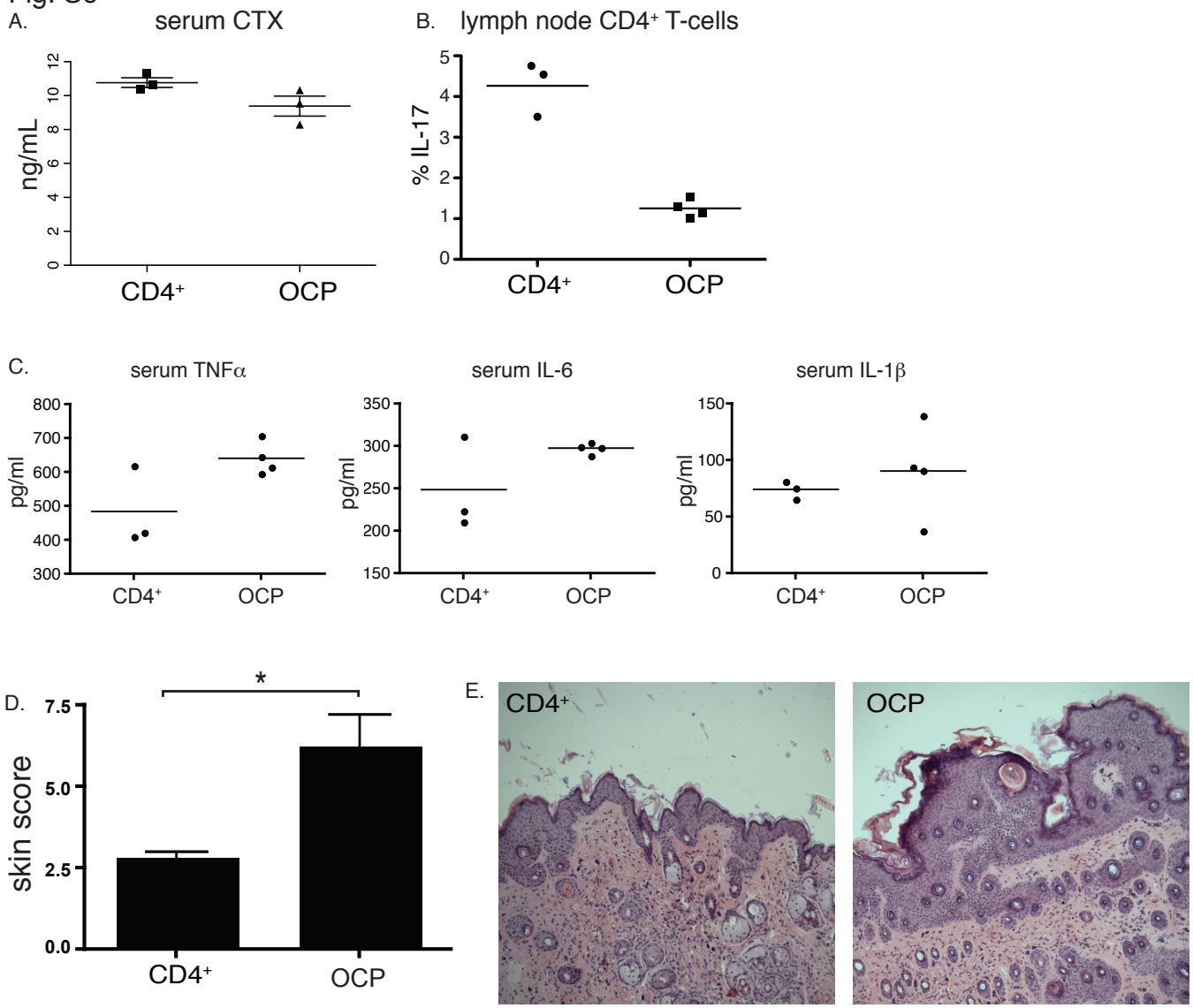

Figure S6. Co-adoptive transfer of CD11b$^{-/lo}$ Ly6C^{hi} OCP does not alter serum CTX, nor decrease inflammatory cytokines. (A) Serum CTX measuered by ELISA. (B) Despite amelioration of inflammatory arthritis, serum levels of TNFα, IL-6 and IL-1 are not significantly reduced in mice receiving co-adoptive transfer of OCP. **(C)** IL-17 producing CD4$^+$ lymp node T-cells are decreased in the OCP group, but serum IL-17 levels are unchanged (data not shown), **(D)** Co-transfer of OCP significantly exacerbates inflammatory skin lesions compared to adoptive transfer of SKG CD4$^+$ T-cells alone, *p= 0.03 Student's t-test. The T_{reg} group had no skin abnormalities. **(E)** Represenative images of skin pathology shows shows acanthosis, hyperkeratosis and dermal infiltrates that are more pronounced in the OCP group comparted to the CD4$^+$ group. H&E stain, 4X.

Fig. S7

A.

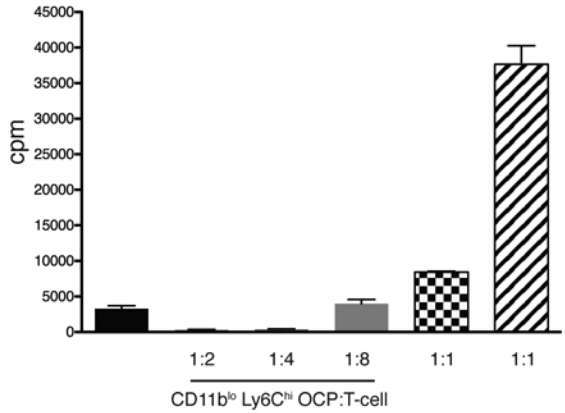

Fig. S7. A. CD11b^{lo} Ly6C^{hi} OCP suppress *in vitro* CD8^{+} T-cell proliferation. CD11b^{lo} Ly6C^{hi} OCP purified from SKG bone marrow suppress CD8^{+} T-cell proliferation (gray bars) in contrast to CD11b^{+}Ly6C^{int} (checked bars) or QN (striped bars) populations from the same bone marrow. Data is representative of 2 independent experiments.